Ionization Relaxation in a Closed-Cycle MHD Generator

C. A. Borghi* and A. Veefkind†
Eindhoven University of Technology, Eindhoven, the Netherlands

The onset of the nonequilibrium conductivity in a closed-cycle MHD generator is experimentally investigated. Conditions for deviations from a Maxwellian electron energy distribution are realized during an afterglow experiment. Here values of the electron temperature and electron density correspond with those present at the entrance of an MHD generator working at low stagnation temperatures ($T_S \leq 2000$ K). Minimum currents are measured in MHD experiments. They correspond to the threshold values of the electron density ($n_{ec} = 5 \times 10^{18}$ m^{-3}) for the transition from a non-Maxwellian to a Maxwellian shape of the electron energy distribution. For low inlet electron densities ($n_e \leq n_{ec}$) the onset of the nonequilibrium conductivity becomes difficult and relaxation ionization lengths up to the generator length have been shown to exist by the experiments. At low stagnation temperatures, higher inlet values of n_e and shorter relaxation lengths are realized by means of preionization.

I. Introduction

DURING the last few years, work in closed-cycle MHD has been concentrated on the low-temperature regimes (stagnation temperatures $T_S \leq 2000$ K, gas temperature $T_g \leq 1000$ K). The MHD conversion in closed-cycle generators is realized through the nonequilibrium conductivity characterized by an electron temperature higher than the gas temperature. For low gas temperatures, long ionization relaxations (necessary to achieve the nonequilibrium) have been shown by experimental investigations.[1]

Neither one- nor two-dimensional calculations[2-5] can explain the long relaxation lengths (length between the first loaded electrode pair and the position where the current is 0.63 times its maximum) observed in linear generators. The two-dimensional calculations predict relaxation lengths of a few centimeters up to the channel height, whereas relaxation regions with lengths up to the generator length have been observed. These models assume a Maxwellian electron energy distribution. In Ref. 6 a model of an Ar-Cs stationary discharge is described. The model takes into account the possibility of deviations from the Maxwellian electron distribution. The electron distribution is described by two Maxwellian functions: one for the electrons with energy lower than 1.43 eV (bulk electrons) characterized by a temperature T_e, and one for the electrons with energy larger than 1.43 eV (tail electrons) characterized by a temperature T_t. A non-Maxwellian distribution with an underpopulated tail ($T_e > T_t$) is calculated for electron densities of the order of those present in the inlet of the generator working at a low stagnation temperature. When a non-Maxwellian electron distribution is taken into account, calculations of the relaxation processes yield an increased ionization relaxation time.[7]

The aim of the present experimental investigation is twofold: first, to see whether a non-Maxwellian distribution can affect the plasma at the low electron densities present at the generator inlet and, second, to see whether a non-Maxwellian distribution can be the cause of the observed long relaxation lengths. In order to answer the first question, an afterglow experiment has been set up. This has been done because of the difficulty of performing detailed measurements in an MHD generator. The MHD generator experiments are then described. The experimental results are analyzed by means of the non-Maxwellian theory developed in Refs. 6 and 7.

II. Decay Relaxation in an Ar-Cs Plasma

In this section an afterglow experiment in an Ar-Cs mixture is described. The aim is to obtain information on the plasma behavior at low electron densities ($n_e < 10^{20}$ m^{-3}).

The experiment is carried out in a Pyrex glass tube with a diameter of 1 cm.[8] The filling pressure at room temperature is 200 Torr. This corresponds to an argon density of 6.6×10^{24} m^{-3}. During its operation, the tube is kept at a temperature $T_w = 520$ K. Hence the density of cesium, determined by the saturation pressure of the vapor of cesium at T_w, is 7×10^{21} m^{-3}. After a stationary discharge of 2 A, the electrodes are externally short circuited. The discharge current drops from 2 to 0.07 A in a time of 2 μs and then decreases slowly to zero, usually in 10 ms.

The intensities of continuum recombination radiation and of line radiation are measured during the afterglow. The continuum radiation observed lies between 4000 and 5000 Å. It is caused by recombinations of Cs^+ ions with electrons of energy range of 0-0.89 eV. The electron temperature and the electron density are derived from continuum radiation data.[9] Hence they refer to bulk electrons. The observed line radiation corresponds to the transition $6P_{3/2} \rightarrow 6S_{1/2}$ of the Cs atom. From the measured light intensity the population of the $6P$ state is derived.

In Fig. 1 the decay of the electron temperature T_e is shown. T_e decreases during the first 100 μs down to about 1200 K. This value approximates the gas temperature in the axis of the discharge, as can be estimated from the energy balance of the gas.[9] The decay of the electron density n_e and the decay of the population density of the $6P$ level n_{6P} are plotted in Fig. 2. From the measured T_e, n_e, and n_{6P}, the energy gain P_{2l}^t and the Coulomb energy transfer P_C^{bt} are derived using the formulation of Ref. 6. The values obtained are plotted as a function of time in Fig. 3. P_{2l}^t stands for the energy released in the cloud of the tail electrons by the de-excitations from the $6P$ to the $6S_{1/2}$ state. P_C^{bt} stands for the energy transfer due to the electron-electron interactions from the bulk electrons to the cloud of the tail electrons. When the two terms are of the same order, a deviation from the Maxwellian electron energy distribution is to be expected.[6] In the first 40 μs, P_C^{bt} is sub-

Received Nov. 23, 1982; revision received June 23, 1983.

*Staff Scientist, Division Direct Energy Conversion, Department of Electrical Engineering; presently with Istituto di Elettrotecnica, University of Bologna, Italy.

†Staff Scientist, Division Direct Energy Conversion, Department of Electrical Engineering.

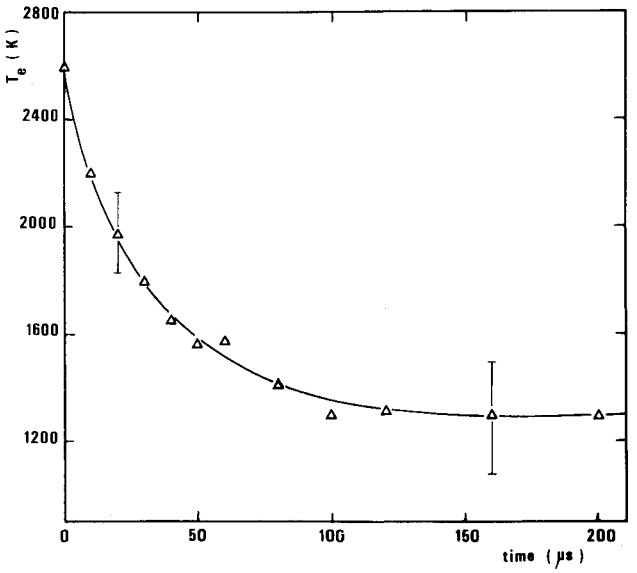

Fig. 1 Decay of the electron temperature.

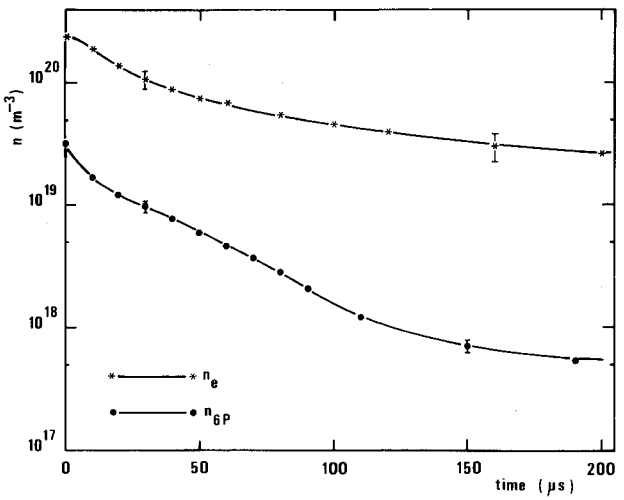

Fig. 2 Decay of the electron density and of the population density of the $6P$ state of cesium.

stantially larger than P_{21}^t, so that the energy gained from the de-excitations is spread out over the electron energy distribution due to the electron-electron interactions. Hence, it is to be expected that for this part of the afterglow the electron distribution remains Maxwellian. For $t>40$ μs, P_C^{bt} and P_{21}^t are of the same order. For this part of the afterglow, the electron-electron interactions are not efficient enough for the transfer of the de-excitation energy. Consequently, the distribution function becomes overpopulated in the tail.

III. Relaxation in an MHD Generator

In this section an experimental investigation of the ionization process in a noble gas MHD generator is described. The experiments are carried out in the shock tunnel MHD facility described in Ref. 10. An Ar-Cs mixture is used as the test gas. The stagnation pressure is 8 bar and the stagnation temperature 1600-3500 K. From the stagnation region of the shock tube, the test gas flows into the MHD channel through a Mach 2 nozzle. Two channels (1 and 2) have been employed (the reason for this is outside the scope of the present investigation), both of the Faraday type, made of Lexan and having the same dimensions. They have an inlet cross section

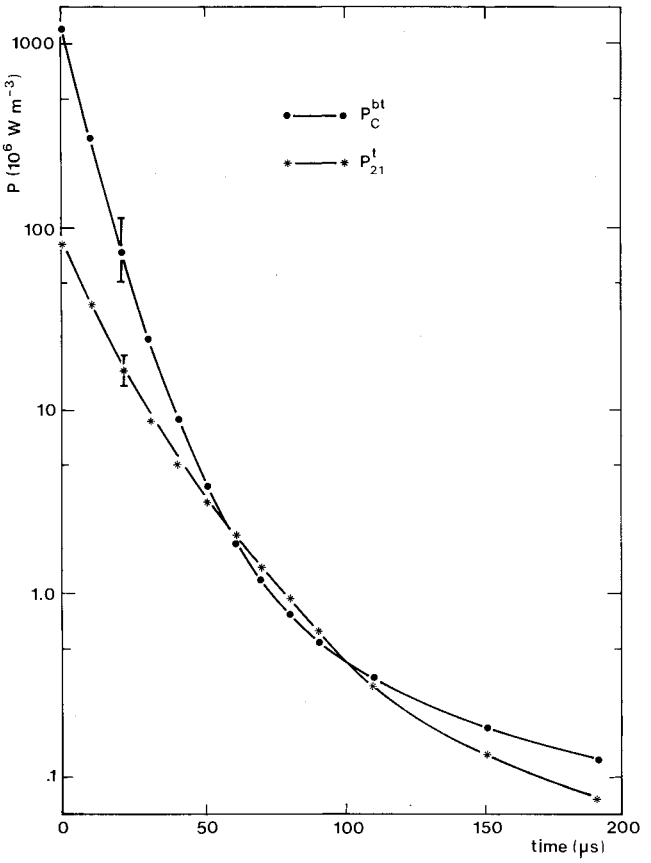

Fig. 3 Comparison of the energy flow term P_c^{bt} due to the electron-electron interactions and the energy gain term P_{21}^t during the afterglow.

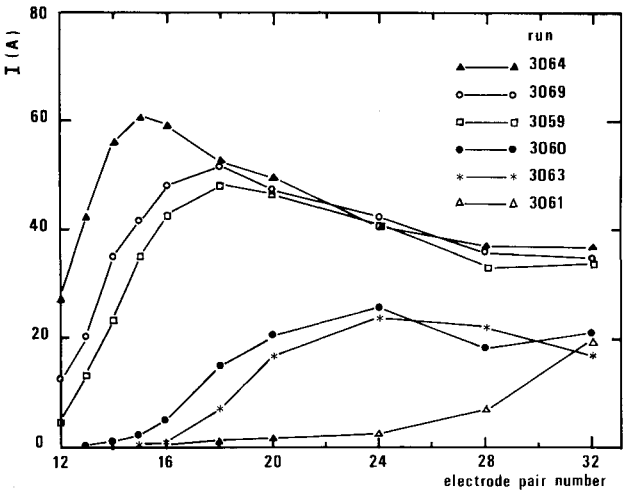

Fig. 4 Current distributions along the channel for some of the runs of Table 1.

of 3.8×11.8 cm^2 and diverge linearly over 80 cm to a cross section of 7.8×11.8 cm^2. The electrodes of both channels are mounted in the parallel walls. Channel 1 has 51 pairs of flat electrodes (width 0.4 cm) mounted flush to the walls. Channel 2 has 32 pairs of cylindrical electrodes (diameter 0.7 cm) half way countersunk into the walls. In both cases, the electrodes are made of stainless steel. Load resistances R_L are separately connected to each electrode pair. The magnetic induction $\boldsymbol{B}$, applied perpendicular to the x-y plane, can reach 3.3 T. A seed ratio $s=[\mathrm{Cs}]/[\mathrm{Ar}]$ of 10^{-3} is used.[11]

Discharge Behavior in the Ionization Relaxation Region

The present investigation is carried out in channel 2. For part of the runs, the electrodes of the pairs upstream of the 12th have not been connected and the electrodes of the pairs from the 12th to 32nd are each connected to a load resistance of 2 Ω. This has been done in order to establish the relaxation region in front of the largest port of the channel. For the other runs, a load resistance of 2.26 Ω is used for each electrode pair.

Electrical currents, Hall voltages, and static pressures are measured. In order to study the development of the discharge in the relaxation region, high-speed photography in the framing and streak modes has been employed. Framing pictures of five complete electrode segments have been made. A sequence of eight pictures is taken in an interval of 35 μs. The exposure time for each frame is 1 μs. For the streak photography, a slit is projected on the center of the channel parallel to the flow direction.[9] It covers 20 cm between the 12th and the 20th electrode pair. The streak velocity, directed along the y direction, is about 140 m/s.

A number of runs with different parameters, leading to different relaxation lengths L_R have been made. The values of L_R and the main gasdynamic parameters are shown in Table 1. L_R is obtained from the measured current distribution along the channel. The gas pressure p_g, the gas temperature T_g, and the gas velocity u_g indicated in the table refer to the position at the 16th electrode pair. The value of p_g is measured at that location. T_g and u_g are calculated by using a one-dimensional gasdynamic program.[9] The values of the magnetic induction, the thermal power input P_{th}, and the electrical power output P_{el} are also listed in the table. Current distributions along the channel are given in Fig. 4. From the figure, it can be seen that the relaxation length increases both with the decrease of the stagnation temperature and with the decrease of the magnetic induction.

In Fig. 5 the discharge structure shown by frame photography is presented. The discharge is strongly inhomogeneous in the relaxation region (Fig. 5a), as well as downstream of the relaxation region (Fig. 5b). Apparently, the streamers are already formed in the relaxation region. The difference between Figs. 5a and 5b is the downstream bending of the discharges. In the relaxation region, the discharges are displaced over distances comparable to electrode distance h, which is in agreement with the results of two-dimensional calculations.[4] In the downstream area, the bending is substantially smaller. The streamers, however, do not always start from the first electrode, so that the relaxation length can be longer than h.

Streak pictures of the discharge in the relaxation region are shown in Fig. 6. They refer to some of the runs listed in Table 1. The discharge is everywhere constricted in streamers. The streamers flow with a velocity in a first approximation equal to the gas velocity (see Ref. 12 for further details). The streamers grow by increasing their diameter. Further, this evidence confirms the results of the framing pictures that the streamers do not always start from the first electrode pair. The relaxation length is determined by two processes: the growth of an individual streamer and the characteristic time necessary for the formation of new streamers. However, the characteristic time for the growth of an individual streamer does not depend on the stagnation temperature or on the magnetic induction, whereas the relaxation length depends strongly on these parameters. The comparison of the streak pictures with the current distributions along the generator (Fig. 4) shows that streamers appear as soon as a corresponding minimum current of about 1 A is measured (see runs 3060 and 3063). Taking 1 cm^2 as the characteristic cross-sectional area of the streamer, a current density $J_T \simeq 1 \times 10^4$ A/m^2 corresponds to the minimum current.

Battery Experiment

The nonequilibrium conductivity is built up in the ionization relaxation region. Here the discharge undergoes a transition from a low- to a high-current mode. In order to investigate the current transition, current voltage character-

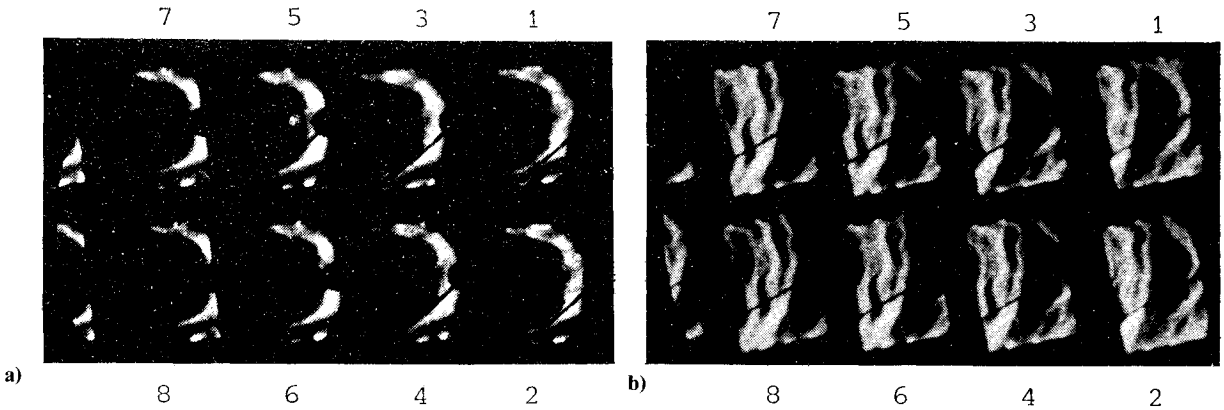

Fig. 5 Framing pictures of the discharge: a) in the relaxation region, b) downstream of the relaxation region.

Table 1 Main parameters of the runs for the investigation of the discharge behavior in the relaxation region

Run	L_R, m	T_S, K	p_S, bar	B, T	T_g, K	p_g, bar	u_g, m/s	P_{th}, MW	P_{el}, kW
3064[a]	0.02	3365	7.27	2.76	1442	0.59	1415	2.9	92.5
3069[a]	0.05	3101	7.80	2.84	1329	0.59	1358	3.0	73.6
3059[a]	0.07	3084	7.23	2.49	1322	0.46	1354	2.8	77.6
3060[a]	0.16	2802	7.32	2.49	1291	0.45	1290	2.7	19.3
3063[a]	0.19	2577	7.36	2.39	1104	0.46	1238	2.6	13.4
3061[a]	0.45	2562	7.33	2.06	1098	0.50	1234	2.0	3.3
2089	0.02	2376	8.24	3.12	1302	0.48	976	2.2	225.0
2086	0.15	2012	8.72	3.00	961	0.39	1011	2.1	117.0
2088	0.55	1762	8.84	3.21	679	0.30	1053	2.1	31.9

[a] Run for which the first 11 electrode pairs are operated under open circuit condition.

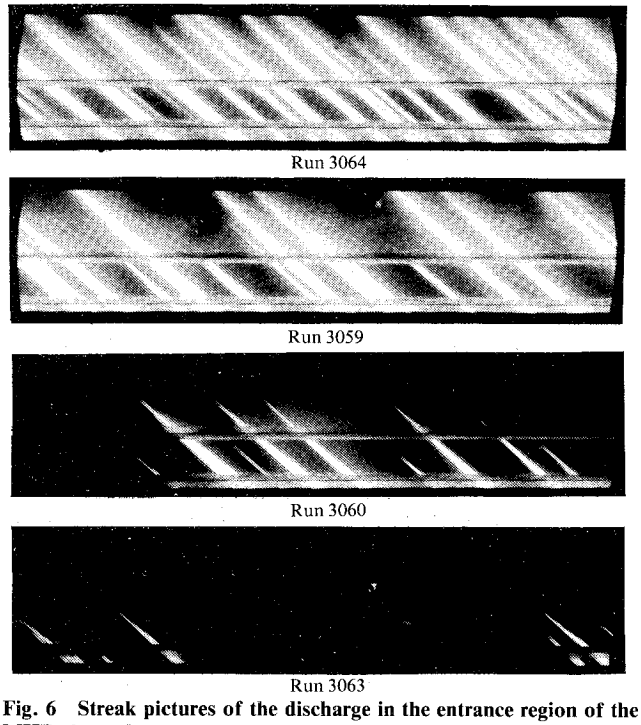

Fig. 6 Streak pictures of the discharge in the entrance region of the MHD channel.

istics of the discharge at one electrode pair have been measured.

The experiments have been carried out in channel 1. The 33rd electrode pair is connected to a set of accumulators in series with a load resistance of 1 Ω. The other electrode pairs are operated under open-circuit conditions. The voltage applied to the plasma V^* is given by $hu_gB+V_b-R_LI$. Here hu_gB is the induced voltage and is derived from the results of the quasi-one-dimensional calculations. V_b is the voltage of the external supply. The current I is derived from the voltage measured over the load.

The experiments are carried out at a stagnation temperature of 3500 K. The static pressure at the 33rd electrode pair is 0.3 bar and the gas velocity is 1500 m/s. Several values of the magnetic induction between 0 and 3 T have been applied.

The resulting I-V^* characteristics are shown in Fig. 7 for several values of the magnetic induction. From the figure it can be seen that a minimum voltage V_T^* is necessary to sustain the discharge. Moreover V_T^* is strongly affected by the magnetic induction. Minimum currents I_T of approximately 2 A are measured. Taking as reference the value of I_T found for $B=0$ and assuming for the discharge cross section the cross section of the generator segment, a current density $J_T=2\times10^3$ A/m^2 corresponds to the minimum current.

Load Resistance Variation

The aim of the experiment described in this section is to examine the relation between the current and voltage in real MHD generators (the applied voltage is now equal to zero). Especially low currents are considered in order to study the onset of the discharge. The induced voltages have been kept constant. The load resistances are varied. All electrode pairs are loaded with the same resistance R_L. By changing the load R_L, an I-V characteristic is obtained. Applied values of R_L are 1, 3, 25, 30, 42, 71, 123 Ω, and ∞. Channel 1 has been used for this experiment. The stagnation temperature is 2400 K, the inlet static pressure 1 bar, and the magnetic induction 2.7 T. The main plasma conditions of each run are listed in Table 2. Here u_g, T_g, and p_g refer to values at the entrance of the generator. The Hall voltage V_H is measured between the 1st and 51st anode. In Fig. 8 the values of the currents are plotted

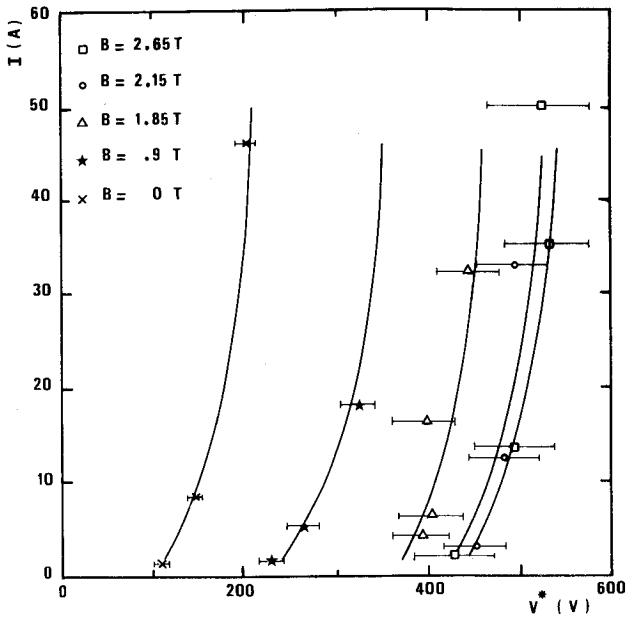

Fig. 7 Current voltage characteristics at several values of the magnetic induction.

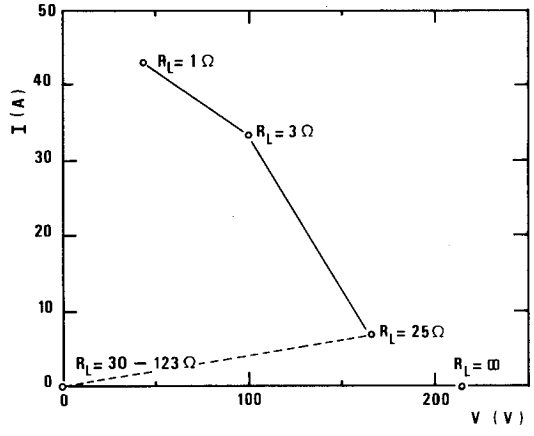

Fig. 8 Current voltage characteristic obtained by variation of the load resistances.

against the measured voltages between the anode and cathode. The currents and voltages indicated in the figure are the averaged values from the 20th up to the 40th electrode pair. For load resistances lower than 25 Ω, the current decreases continuously with increasing R_L, while the voltage increases. For values of R_L between 30 and 123 Ω, the current as well as the voltage become very small. Apparently under these conditions, the nonequilibrium conductivity is not established and the internal resistance is much higher than the load resistance. For $R_L=\infty$ the Faraday open-circuit voltage is measured. As a result of this experiment, it can be concluded that again a transition in the discharge characteristic is found. In this case, the minimum current measured I_T is 6 A. Assuming a constricted discharge with a cross section of 1 cm^2, a current density $J_T=6\times10^4$ A/m^2 corresponds to the minimum current.

Energy Conversion Experiment with Preionization

In order to enhance the conditions for the onset of the nonequilibrium at the inlet of the generator, preionization can be applied. The preionization experiment described in this section is carried out in channel 2. As for the preionization

Table 2 Main parameters of the runs of the experiment with variation of the load resistance

Run	R_L, Ω	T_S, K	B, T	V_H, V	u_g, m/s	T_g, K	p_g, bar	P_{th}, MW	P_{el}, kW
2739	1	2390	2.55	570	1043	1024	1.19	3.3	78
2740	3	2320	2.82	471	1136	994	1.16	3.6	122
2745	25	2432	2.65	381	1210	1042	1.09	3.5	42
2749	123	2400	2.80	302	1200	1012	1.13	3.5	0
2742	∞	2432	2.20	181	1260	1042	1.19	3.7	—

Table 3 Parameters corresponding to the characteristic currents observed in the experiments of Sec. III

Experiment type	J, 10^4 A/m^2	E, 10^3 V/m	σ, S/m	n_e, 10^{18} m^{-3}
Battery	0.2	0.9	2	2
R_L variation	6	2.0	30	33
Relaxation	1	2.9	4	4
Preionizer	2.2	1.5	15	16
2nd electrode pair	5	2.3	20	21

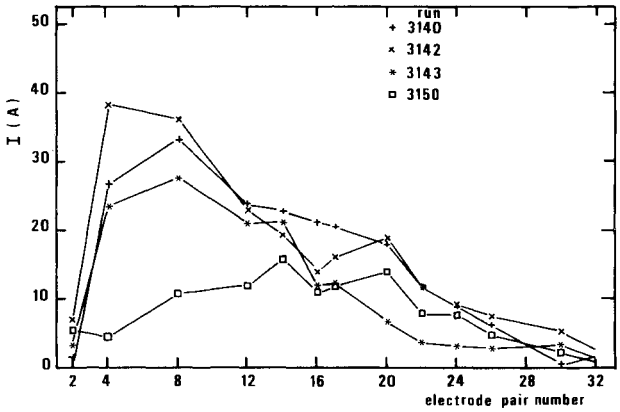

Fig. 9 Current distributions along the channel in the preionization experiment.

system, a power supply is interconnected between the first electrode pair and the stagnation region of the shock tube. Load resistances of 1 Ω are used. The magnetic induction is 2.5 T, the gas pressure 0.65 bar, and the gas velocity 1000 m/s. The electrode current distribution along the generator for each run is shown in Fig. 9. Nonequilibrium conductivity is realized in a run at a stagnation temperature as low as 1610 K, whereas the minimum stagnation temperature at which an appreciable MHD conversion is realized in previous experiments is 1762 K (compare Table 1). The preionization current used to realize the nonequilibrium conductivity at $T_S = 1610$ K is 99 A. As the preionization current is along the flow direction outside of the magnet, it is assumed that the preionization current fills the whole generator cross section at its entrance. Hence, a corresponding current density $J = 2 \times 10^4$ A/m^2 is calculated. The current at the second electrode pair is perpendicular to the magnetic induction and a discharge cross section of 1 cm^2 is assumed. Thus, a current density $J = 5 \times 10^4$ A/m^2 corresponds to the current measured here.

IV. Discussion

Conditions for deviations from the Maxwellian electron energy distribution are observed during the afterglow experiment described in Sec. II. For low values of n_e ($\lesssim 10^{19}$ m^{-3}) the electron-electron interactions are insufficient to thermalize the energy gained by the tail electrons due to the de-excitations from the first excited state. Consequently, the tail of the electron distribution becomes overpopulated. Because the values of T_e and n_e in the inlet region of the MHD generator are of the same order as realized during the afterglow, deviations from the Maxwellian shape of the electron energy distribution have to be expected there as well. During the ionization of the plasma, the energy loss caused by the excitation to the first excited state of cesium is not thermalized by the electron-electron interactions and the tail of the electron distribution becomes depleted.

The values of the current density corresponding to the minimum currents measured in MHD experiments are listed in Table 3. In this table the values derived from the preionization current and from the current of the second electrode pair (the first electrode pair is used for the preionization system) in the preionization experiment at 1610 K are also indicated. For all experiments the electric field E is derived from $V^* = hu_gB + V_b - R_L I$. The value of the electrical conductivity is obtained as J/E. The electron density is then derived from σ by assuming the momentum collision frequency between the electrons and heavy particles equal to 3×10^{10} s^{-1} (value corresponding to $T_e = 2000$ K). The value of n_e has only an indicative meaning due to the lack of information of the inhomogeneous structure of the plasma in the generator at low electron density. Table 3 shows that the values of n_e corresponding to the minimum currents approximate or are larger than n_{ec} ($n_{ec} = 5 \times 10^{18}$ m^{-3}), which is given by the theory as the threshold for the Maxwellian regime.[6] Hence, an indication is found that the minimum current density observed in the MHD generator experiments is related to the transition from a non-Maxwellian to a Maxwellian regime. An electron density higher than n_{ec} is obtained, for instance, by means of the preionizer. Here, the high current regime is already present at the inlet of the generator. Therefore, the generator can work under conditions where Maxwellian electron distribution can be expected and thus a nonequilibrium state can be built up.

In Table 1 for a stagnation pressure of 8.5 bar, a magnetic field of 3 T and stagnation temperatures of 2400, 2000, and 1800 K, relaxation regions of 2, 15, and 55 cm are shown, respectively. Correspondingly, electron densities of 3.6×10^{20}, 4.8×10^{19}, and 1.3×10^{19} m^{-3} are obtained in the stagnation region of the shock tube. These values lead to electron densities of 4.5×10^{19}, 5.9×10^{18}, and 1.6×10^{18} m^{-3} at a pressure of 1 bar in the entrance region of the MHD generator. In the first case ($T_S = 2400$ K) the inlet electron density is larger than n_{ec} and the discharge develops from a Maxwellian initial condition. The nonequilibrium conductivity is easily built up. For the second case ($T_S = 2000$ K), the inlet electron density is about equal to the critical electron density n_{ec} where the transition between the non-Maxwellian and Maxwellian regimes is expected. The onset of the discharge is more difficult than in the former case, but the nonequilibrium regime can still be built up in a reasonable distance from the inlet of the generator. However, when the inlet n_e is smaller than n_{ec} ($T_S = 1800$ K), the onset of the nonequilibrium regime becomes critical. Below 1800 K it is not possible to obtain a sufficient nonequilibrium conductivity without increasing the inlet electron density by means of preionization.

V. Conclusions

Conditions for deviations from a Maxwellian distribution are observed during an afterglow experiment. For low electron densities ($n_e \lesssim 10^{19}$ m^{-3}) the electron-electron interactions are not efficient enough to thermalize the electron energy realized by the nonelastic interactions. As the range of the electron temperature and electron density in the entrance region of an MHD generator are the same as that realized during the afterglow, deviations from the Maxwellian shape of the electron distribution have to be expected here as well.

Minimum values of the current are measured in MHD generator experiments. They correspond to the electron density for which a transition from non-Maxwellian to Maxwellian electron distribution is predicted by the theory. When the electron distribution is non-Maxwellian, the onset of the nonequilibrium becomes difficult. Hence, the ionization relaxation process is retarded and leads to the long relaxation lengths shown by the experiments.

By means of preionization an increase of the inlet electron density is realized and better conditions for the onset of the nonequilibrium are obtained.

Acknowledgments

This work was performed as part of the research program of the Division Direct Energy Conversion of the Eindhoven University of Technology, Eindhoven, the Netherlands. It was supported by the Commission of the European Communities, the Eindhoven University of Technology, and the CNR-Ufficio Relazioni Internazionali (Italy). The authors wish to express their gratitude to Prof. dr. L. H. Th. Rietjens and Prof. dr. J. F. Uhlenbusch for their contribution and fruitful discussions. The technicians of the Shock Tube MHD Project are thanked for their technical assistance.

References

[1] Veefkind, A., Hellebrekers, W. M., Borghi, A. A., and Rietjens, L. H. Th., "Noble Gas MHD Generator Experiments at Low Stagnation Temperature," *Proceedings of the 17th Symposium on Engineering Aspects of MHD*, Stanford, Calif., 1978, Paper H.3.

[2] Bertolini, E., Toschi, R., and McNab, I. R., "Relaxation Phenomena in MHD Generators," *Proceedings of the 3rd International Symposium on Magnetohydrodynamic Electrical Power Generation*, Vol. 1, Salzburg, 1966, pp. 533-545.

[3] Takeshita, T. and Grossman, L. M., "Excitation and Ionization Processes in Non-Equilibrium MHD Plasmas," *Proceedings of the 4th International Symposium on Magnetohydrodynamic Electrical Power Generation*, Vol. 1, Warsaw, 1968, pp. 191-206.

[4] Blom, J. H. and Houben, J. W. M. A., "Relaxation Length Calculations in Ar-Cs Mixtures for One- and Two-Dimensional Pre-Ionizer Geometries," *Proceedings of the 5th International Conference on Magnetohydrodynamic Electrical Power Generation*, Vol. 2, Munich, 1971, pp. 65-79.

[5] Hara, T., Veefkind, A., and Rietjens, L. H. Th., "A Numerical Investigation of the Inhomogeneous Discharge Structure in Noble Gas MHD Channels," *Proceedings of the 19th Symposium on Engineering Aspects of MHD*, Tullahoma, Tenn., 1981, Paper 7.2.

[6] Borghi, C. A., "Model of the Stationary Discharge in Noble Gas MHD Generator Plasmas at Low Electron Densities," *Physica*, Vol. 119C, April 1983, p. 351.

[7] Borghi, C. A., Veefkind, A., and Wetzer, J. M., "Effect of Radiation and Non-Maxwellian Electron Distribution on Relaxation Processes in an Atmospheric Cesium Seeded Argon Plasma," *Physica*, Vol. 120C, July 1983, p. 269.

[8] Borghi, C. A. and Flinsenberg, H. J., "Experimental Investigation of a Steady-State Arc Discharge in an Ar-Cs MHD Generator Plasma," *Proceedings of the 15th International Conference on Phenomena in Ionized Gases*, Vol. 1, Minsk, 1981, pp. 329-330.

[9] Borghi, C. A., "Discharges in the Inlet Region of a Noble Gas MHD Generator," Ph.D. Thesis, Eindhoven University of Technology, Eindhoven, the Netherlands, 1982.

[10] Veefkind, A., Houben, J. W. M. A., Blom, J. H., and Rietjens, L. H. Th., "High-Power Density Experiments in a Shock-Tunnel MHD Generator," *AIAA Journal*, Vol. 14, Aug. 1976, pp. 1118-1122.

[11] Veefkind, A., Sens, A. F. C., and Wetzer, J. M., "Shock Tube Investigations on MHD Conversion in Argon-Cesium," *Proceedings of the 19th Symposium on Engineering Aspects of MHD*, Tullahoma, Tenn., 1981, Paper 7.3.

[12] Sens, A. F. C., Bityurin, V. A., Wetzer, J. M., and Veefkind, A., "Investigations on the Gasdynamical Effects of a Non-Uniform Supersonic Flow with Streamers in a Noble Gas MHD Generator," *Proceedings of the 20th Symposium on Engineering Aspects of MHD*, Irvine, Calif., 1982, Paper 10.6.